Presented at the 32nd European PV Solar Energy Conference and Exhibition, 20-24 June 2016, Munich, Germany

ENABLING SOLDERABILITY OF PVD AL REAR CONTACTS ON HIGH-EFFICIENCY CRYSTALLINE SILICON SOLAR CELLS BY WET CHEMICAL TREATMENT

H. Nagel, M. Kamp, D. Eberlein, A. Kraft, J. Bartsch, M. Glatthaar and S. W. Glunz

Fraunhofer Institute for Solar Energy Systems (ISE), Heidenhofstraße 2, 79110 Freiburg, Germany
Email: henning.nagel@ise.fraunhofer.de

ABSTRACT: Results of an electroless displacement process for the deposition of inexpensive solderable metal on physical vapour deposited (PVD) aluminum are presented. The dip – rinse – dry processing sequence for electroless metal deposition on Al is simple and easy to use because it does not harm the SiN antireflection coating and the screen-printed Ag metallization on the cells' front side. Hence, finished cells can entirely be immersed into the electrolyte. The deposited metal layer is highly porous, but forms a massive alloy with common Sn/Pb/Ag solder at low temperature of 245 °C in the presence of no-clean flux. Because the molten alloy wets Al and copper well, we obtained strong solder joints for Sn/Pb/Ag coated copper ribbons on Al. The measured average 90° peel forces of ribbons soft soldered to thermally evaporated Al on shiny etched silicon and on the rear of alkaline textured monocrystalline Si PERC solar cells were up to 3.1 and 2.2 N per mm ribbon width, respectively. These values exceed 1 N/mm that is specified by the standard DIN EN 50461. Climate tests on single-cell glass-glass modules yielded 4.1 and 7.7 % power degradation after 200 thermal cycles from -40 °C to 85 °C and after 1000 h under damp-heat conditions at 85 °C and 85 % relative humidity, respectively. We attribute the too high power degradation after damp-heat test to residuals of the acidic flux which was used for soldering the cells in this first, older version of the developed technology.

Keywords: Evaporated Aluminum, Electroless Deposition, Cell Interconnection

1 INTRODUCTION

At present, most industrial crystalline silicon solar cells feature screen-printed rear contacts that consist of large-area Al and local Ag solder pads. During sintering of the printed pastes the Al alloys with the Si and forms a highly doped *p*-type back surface field (BSF) which is well suited for common *p*-type c-Si cells. However, printed and sintered Al rear contacts suffer from several shortcomings:

i) Thin dielectric passivation layers (like e. g. Al_2O_3) on the back of passivated emitter and rear cells (PERC) have to be protected against the printed Al by means of a capping layer (usually SiN) in order to avoid spiking of Al through the passivating film.

ii) Possible degradation of the rear surface passivation even with capping layer present due to the high sintering temperature.

iii) Increased effective surface recombination velocity in comparison to boron BSF made by other methods.

iv) Damage of *n*-doped BSF on *n*-type cells.

Hence, high-efficiency c-Si solar cells usually rely on physical vapor deposited (PVD), i. e. evaporated or sputtered, Al. It makes good ohmic contact to *p*- and *n*-type Si, provides excellent back reflection of weakly absorbed infrared light passing through the cells and features very high electrical conductivity. Good examples for c-Si solar cells featuring PVD Al rear contacts are *n*-Q.ANTUM cells presented by Hanwha Q-Cells which yielded efficiencies above 21 % [1] and the 'PassDop' cells introduced by Fraunhofer ISE which reached efficiencies up to 23.5 % on small area [2] and above 22 % on large area [3]. However, a technical challenge that is associated with PVD Al rear contacts is the series connection of the solar cells to strings. The interconnect ribbons cannot be directly soldered to the base metal aluminum because in ambient atmosphere it is covered by a very quickly formed dense Al_2O_3 film that is about 2.5 nm thick. Solutions which were already proposed for this problem have distinct pros and cons in terms of feasibility and cost:

In [4,5,6], solderable metal stacks were vacuum deposited on Al. The stacks TiN/Ti/Ag, NiV/Ag und NiSi/Ag on Al yielded high peel forces of soldered interconnect ribbons. The layers can be vacuum deposited in the same deposition system in a single pass without venting, but the costs are relatively high because several vacuum chambers and different installations for thermal evaporation and sputtering are needed in the deposition system.

A well known modification of this technique is the metallization scheme developed by Sunpower Corp. for rear-contacted c-Si solar cells [7]. Here, PVD Al is sputter coated with a TiN or TiW adhesion layer which is subsequently electroplated with copper and tin. The adhesion layer simultaneously acts as a barrier against diffusion of copper through the aluminum into the silicon substrate. This technique greatly reduces the amount of vacuum deposited metal for cost reasons but relies on electroplating equipment.

A plating-based approach was also investigated in [8]. In a first step, the aluminum is immersed in an alkaline zincate solution. Then, the deposited zinc layer is etched off in order to obtain a roughened surface and to increase the surface area. Subsequently, zinc is re-deposited in a second zincate step followed by electroplating of a Ni/Cu/Ag stack. Here, the thin plated nickel layer acts as adhesion promoter and diffusion barrier against copper. Interconnect ribbons soldered on this metal stack yielded high peel forces exceeding 1 N/mm on an average.

In [9,10] it was proposed to apply a tin coating on the aluminum rear contact by ultrasonic soldering. High-throughput systems for production of these so-called tin pads on large-area cells are available [11]. Onto tin pads interconnect ribbons can be soft soldered in standard tabber stringers. No flux is needed and no expensive metals are consumed. The technique was developed for screen-printed aluminum. Probably it is suited for PVD Al as well. However, to the best of our knowledge there is no publication

about the application to PVD Al, yet.

There are more joining technologies for aluminum, for example welding and hard soldering. We expect that they are not well suited for solar cell interconnection because of the involved high substrate temperatures above 450 °C and the associated threat of electrical degradation of the dielectric rear side passivation on PERC cells. A noteworthy exception is laser-welding as demonstrated in [12] for aluminum ribbons on PVD Al. During the laser welding process heat is applied only locally at small spots for a very short time. This way the aluminum foil and the PVD Al can selectively be melted without increasing the temperature of the underlying cell above the degradation threshold. A disadvantage of this process is that special tabber stringers are necessary and that laser welding on PVD Al was only shown for aluminum interconnect ribbons and not for conventional copper ribbons.

In this work we investigated an innovative low-cost approach to make PVD Al solderable. We developed a single wet chemical treatment that deposits inexpensive solderable metal on PVD aluminum.

2 EXPERIMENTAL

Aluminum layers featuring various thicknesses were deposited by high-rate thermal evaporation in an inline vacuum system supplied by Applied Materials Inc. Different substrates were used: shiny etched and alkaline textured silicon wafers and two types of PERC cells. Subsequently, the entire Al coated wafers and cells were dipped in a wet chemical solution for 90 to 180 s at room temperature. At first the used electrolyte etches the native Al_2O_3 layer and then an about 1 µm thick solderable metal (Me) is electroless plated on the Al from the same electrolyte by means of a displacement reaction

$$3\ Me^{n+} + n\ Al \rightarrow 3\ Me + n\ Al^{3+}$$

where n is the chemical valence of the deposited metal. No external electrical contacts were attached to the cells and no external voltage was applied. The driving force for the chemical reaction is the difference in standard electrode potential between Al and the more noble Me. After rinsing and drying, conventional Sn/Ag/Pb-coated Cu ribbons were soldered to the metallization stack by contact soldering. The thickness of the ribbons' copper core and solder coat was 130 µm and about 15 µm, respectively. The ribbons were 2 mm wide and fluxed with widespread Kester 952 s in most of the experiments. The soldering temperature was varied in the range between 245 °C and 400 °C.

From 5 inch 'PassDop' cells mentioned in the Introduction we manufactured single-cell mini-modules featuring soda-lime glass on the front and on the rear. It must be noted that in this experiment we applied the electrolyte on the rear only and that we used a more reactive acidic flux on the ribbons. After soldering at a temperature of 245 °C the flux had to be washed off. The laminated modules were subjected to damp-heat and temperature cycling tests according to the standard IEC 61215.

We studied the microstructure of the films and solder joints by secondary electron microscopy (SEM) and their composition by energy dispersive X-ray spectroscopy (EDX). In order to measure the adhesion of the ribbon soldered on the wafers and cells, an automated 90° peel-force-tester was used. The *IV* curves of cells and modules were measured by means of a flasher system.

3 RESULTS

3.1 Microstructure of the deposited metal layer

The top of Figs. 1 and 2 show plan view SEM images of 3 µm Al thermally evaporated on a shiny etched Si wafer and on an alkaline / random pyramid textured rear of a CZ Si PERC cell, respectively. In the latter case a common surface passivating Al_2O_3/SiN stack was placed between the Si and the Al but in additional experiments we did not observe an effect of these dielectric layers on the microstructure of the Al. It can be seen from the figures, that on shiny etched Si the PVD Al layer consists of 1 to 3 µm large grains and that it uniformly covers the wafer surface. On alkaline textured silicon the PVD Al layer basically reproduces the shape of the random pyramids as well, but the thickness of the Al layer is very non-uniform on a microscopic scale. In the valleys between the pyramids the Al is thin or even missing at small spots, whereas on the tips of the pyramids thick Al crystals are formed, noticeable from their rectangular shape.

After immersion in the electrolyte and rinsing, on both substrates metal layers which essentially consist of separate small particles and a few very large crystallites were found, see bottom of Figs. 1 and 2. The size of the large grains lies in the range between 5 to 13 µm. Without further quantification it is already obvious from the pictures that the porosity of the Me layer on the pyramid textured sample exceed the one on the flat sample.

It can be expected that a highly porous Me layer causes undesired voids in solder joints. In order to shed light on this we electroless deposited Me layers featuring an effective thickness of about 1 µm on each side of an Al foil and soldered Sn/Pb/Ag-coated Cu ribbon at 245 °C on one side. A massive and uniform Al foil was chosen as a substrate instead of a PVD Al coated Si wafer in order exclude the effect of the microstructure of PVD Al in this fundamental

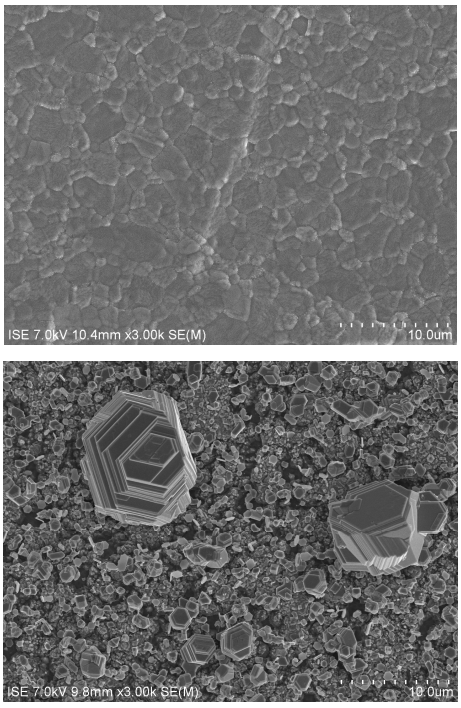

Fig. 1: Plan view SEM picture taken from 3 µm Al thermally evaporated on shiny etched Si before (top) and after (bottom) electroless metal deposition.

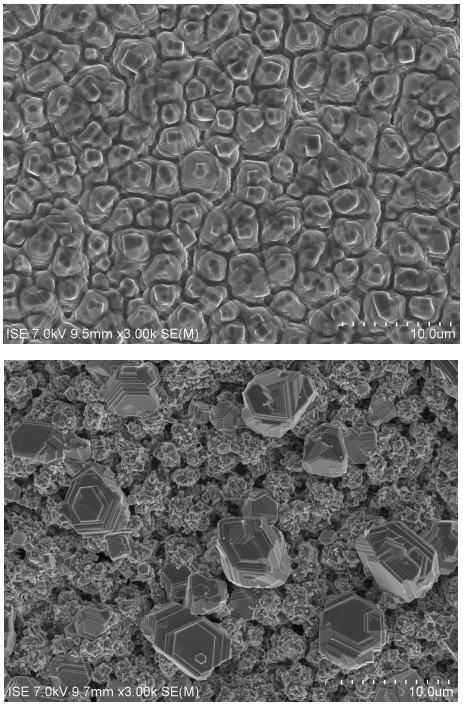

Fig. 2: Plan view SEM picture taken from 3 µm Al thermally evaporated on the Al_2O_3/SiN coated alkaline textured rear side (random pyramids) of a PERC Si cell before (top) and after (bottom) electroless metal deposition.

experiment. Fig. 3 shows the obtained cross-sectional SEM image of the solder joint between Al foil and copper ribbon together with the cross-faded result of the EDX analysis. On top of the Al foil the original porous Me layer can be seen (blue color). Obviously, the area coverage of Me on Al is quite low. Nevertheless, the solder joint region in the center of the image reveals that the Me layer completely alloyed with Sn/Pb/Ag solder. Me is distributed all over the solder, even to the Cu surface. The alloy wets aluminum and copper well which is a prerequisite for the formation of strong solder joints.

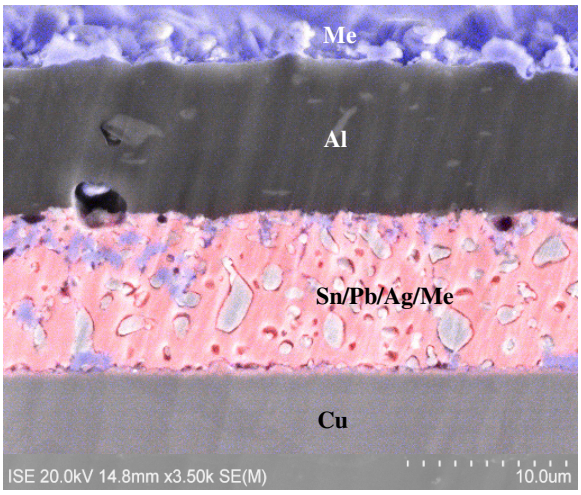

Fig. 3: Cross-sectional SEM picture taken from Al foil electroless coated on both sides with Me and soldered on the bottom side to Sn/Pb/Ag coated Cu ribbon. Cross-faded is an EDX image indicating the concentration of the elements Sn (red) and Me (blue).

3.2 Peel force of soldered interconnect ribbons

1 to 5 µm Al was thermally evaporated on shiny etched and alkaline textured 6 inch CZ Si wafers, respectively. After dipping the wafers for 1 min 45 s into the electrolyte, we soldered interconnect ribbons on the deposited Me layer at a relatively high temperature of 400 °C. The high temperature was chosen because we found that it yields more reproducible results on textured samples. The measured 90 ° peel forces normalised to the ribbon width are shown in Fig. 4 as a function of Al thickness. It can be seen from the figure, that the peel force increases with Al thickness and that there is a trend of the peel force to saturate for thicknesses exceeding 3 µm on alkaline textured Si. Below an Al thickness of 2 µm the peel force significantly drops and approaches zero at 1 µm. The reasons are that about 1 µm Al is dissolved in the electrolyte and the Me layer doesn't adhere to Si but only to Al. In general, the peel force on shiny etched Si is higher compared to alkaline textured Si because the porosity of the Me layer is lower. Independent of surface texture average peel forces of above 1 N/mm were regularly obtained for Al thicknesses exceeding 2 µm which complies with the standard DIN EN 50461.

By optimising the electroless deposition and especially the rinsing process after deposition in order to avoid residual electrolyte on the samples we could further increase the peel forces. Fig. 5 shows the force vs. distance curves for 3 µm Al thermally evaporated on shiny etched Si and on the alkaline textured rear side of a PERC solar cell covered by a common Al_2O_3/SiN passivation stack, respectively. At every location of the wafer and cell the peel force exceeded the desired 1 N/mm. Again, the peel force obtained on the shiny etched wafer was higher compared to the alkaline textured cell. The average peel forces were 2.2 and 3.1 N/mm, respectively. These results imply good adhesion of

a) electroless deposited Me on evaporated Al if the Al thickness is larger than 2 µm

b) evaporated Al on Si

c) evaporated Al on SiN

d) SiN on Al_2O_3 and

e) Al_2O_3 on Si.

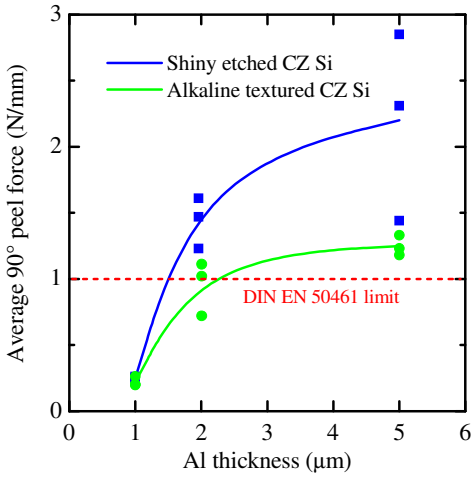

Fig. 4: Average values of the measured interconnect ribbons' 90 ° peel forces of as a function of PVD Al thickness on shiny etched and alkaline textured silicon, respectively. The Al was electroless plated with about 1 µm Me. Lines are guides to the eye.

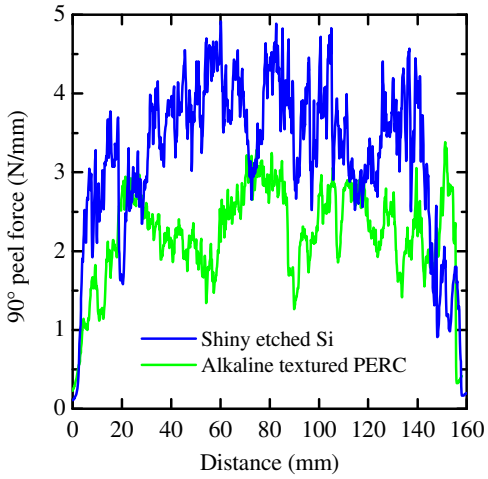

Fig. 5: Measured 90 ° peel force vs. distance curves of Cu ribbons soldered on 3 µm thick PVD Al located on the rear of a PERC c-Si solar cell and on a shiny etched c-Si wafer, respectively.

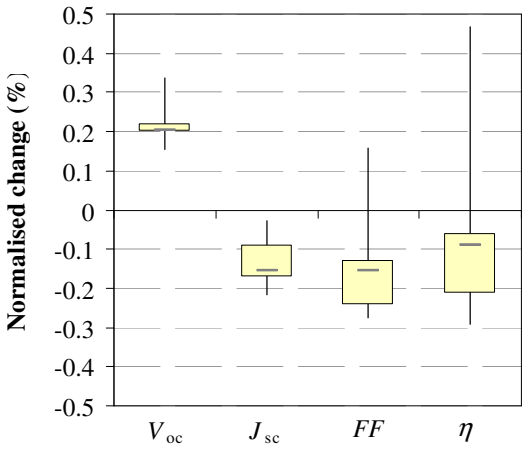

Fig. 6: Measured normalised change of electrical performance parameters caused by immersing entire cells in the electrolyte.

3.3 Impact of electrolyte on solar cell efficiency

If desired, electroless metal deposition can solely be applied on the cells' rear side by means of state-of-the-art high-throughput inline systems which are available for electroplating or for rear side etching. In this production-type equipment the cells move horizontally above the electrolyte, e. g. on rollers that are arranged in a row. The rollers are partially immersed in the wet chemical solution so that they transport the electrolyte to the rear of the cells during rotation. However, in some other cases batch processing is desired. It offers high throughput with small equipment footprint because a large number of cells are processed simultaneously. In the lab it might be the handling of choice because no inline wet bench is available.

Batch processing is associated with placing a large number of cells vertically in a carrier and immersing the entire carrier at once in the electrolyte. Inevitably both, PVD Al rear contact and front metal grid are exposed to the electrolyte if the latter was deposited before. This is generally the case for common screen-printed and fired front metallization because of the high thermal budget which would counteract the advantages of the PVD Al as described in the Introduction. Hence, we investigated the effect of the electrolyte on 6 inch *p*-type CZ Si PERC cells featuring screen-printed Ag front side metallization and SiN antireflection coating. Both sides were alkaline textured and the rear was coated by an Al_2O_3/SiN surface passivating layer stack. 3 µm Al was thermally evaporated on the rear and local back-surface fields were prepared by laser contact firing of the Al after deposition. The entire cells were dipped for 1 min 45 s in the electrolyte, rinsed and dried. *IV* curves were measured before and after dipping. Fig. 6 shows the measured change of electrical performance parameters normalised to the values before electrolyte exposure. It can be seen from the figure, that the median normalised efficiency (η) reduction was 0.1 % which transfers to less than 0.02 % absolute for these cells that feature a maximum efficiency of 20.1 %. Considering the small number of only 5 cells used in this experiment and the measurement uncertainty we conclude that the obtained small change is within the experimental error and hence neither SiN antireflection coating nor screen-printed front metal grid are harmed by the electrolyte. The latter is further supported by the fact that there was no change of measured finger resistance on the front side. However, as expected, we observed an increase of the rear contacts' sheet resistance from 11 to 13 mΩ. It corresponds to a reduction of Al thickness from 3 to 2.4 µm assuming that the conductivity of the deposited porous metal layer can be neglected. From this, the analytical calculation of the resistive power loss taking into account the used 3 busbar design yielded an efficiency reduction of 0.04 % relative.

3.4 Results of first climate tests

We manufactured two single-cell glass-glass modules from 5 inch *n*-type CZ Si 'PassDop' PERC cells featuring alkaline textured front side and shiny etched rear side, Ni/Cu/Ag plated front contact, SiN antireflection coating, phosphorous doped passivating SiN on the rear underneath about 2.5 µm thermally evaporated Al. In this case we locally deposited solderable Me only on the areas where the interconnect ribbons were soldered on the rear Al. Furthermore, we applied a strong acidic flux to the interconnect ribbons before soldering at 245 °C in order to guarantee good wetting of the Me. After soldering, the ribbons were cleaned, i. e. the flux was washed off. Table 1 shows the measured change of electrical performance parameters after damp-heat (DH) test at 85 °C, 85 % relative humidity for 1000 h and after 200 thermal cycles (TC) at temperatures from -40 °C to 85 °C. These climate tests were performed according to IEC 61215 standard. Whereas the TC test was passed (efficiency degradation was lower than 5 % relative), normalized efficiency reduction after DH test was 7.7 % mainly due to a decrease of *FF*. We attribute it to residuals of the acidic flux which presumably were not completely washed off. Hence, no-clean flux should be used as we did in the study for optimization of the peel force.

Table 1: Measured change of electrical performance parameters of single-cell glass-glass modules containing 5 inch 'PassDop' cells after temperature cycling (TC) and damp-heat (DH) test.

Test	$\Delta V_{oc}/V_{oc}$ (%)	$\Delta J_{sc}/J_{sc}$ (%)	$\Delta FF/FF$ (%)	$\Delta\eta/\eta$ (%)
TC	-0.6	-0.9	-2.7	-4.1
DH	-0.6	-0.8	-6.4	-7.7

4 SUMMARY

We developed an electroless displacement process for the deposition of solderable metal on PVD Al. By a simple dip – rinse – dry processing sequence about 1 µm of Al is dissolved in the electrolyte and at the same time a Me layer featuring an average thickness of about 1 µm is deposited. Although the microstructure of the Me layer is highly porous, the adherence to PVD Al is good. Already at a temperature of 245 °C the metal uniformly alloys with standard Sn/Pb/Ag solder using common no-clean flux. Because the alloy wets Al and copper well, we obtained strong solder joints on thermally evaporated Al. By an optimised process we achieved average 90° peel forces of 2.2 N/mm on the rear of PERC cells and of 3.1 N/mm on shiny etched Si. These values are well above 1 N/mm which is specified by the standard DIN EN 50461. In combination with SiN antireflection coating and screen-printed Ag metallization on the front side the electroless displacement process is suited for batch handling because the electrolyte does not harm the solar cells' front side. First climate tests on single-cell glass-glass modules containing 'PassDop' cells yielded 4.1 and 7.7 % power degradation after 200 thermal cycles and 1000 h damp-heat test. We attribute the too high power degradation after damp-heat test to residuals of the non-standard acidic flux which was used for soldering in this first, older version of the developed technology.

ACKNOWLEDGEMENT

The authors thank all colleagues at Fraunhofer ISE who contributed to this work and the German Federal Ministry for Economic Affairs and Energy for funding within the projects 'IdeAl' under contract number 0325889B and 'rEvolution' under contract number 0325586B. The excellent co-operation of the project partners is gratefully acknowledged.

REFERENCES

[1] V. Mertens, T. Ballmann, J. Cieslak, M. Kauert, A. Mohr, F. Stenzel, M. Junghänel, K. Suva, C. Klenke, G. Zimmermann, J. Müller, *Proceedings of the 28th European Photovoltaic Solar Energy Conference* (2013) 714.

[2] B. Steinhauser, M. Kamp, J. Bartsch, A. Brand, J. Benick and M. Hermle, *Proceedings of the 6th World Conference on Photovoltaic Energy Conversion* (2014).

[3] B. Steinhauser, M. Kamp, A. Brand, U. Jäger, J. Bartsch, J. Benick and M. Hermle, IEEE J. of Photovoltaics (2016) 419.

[4] J. Kumm, H. Samadi, P. Hartmann, S. Nold, A. Wolf and W. Wolke, *Proceedings of the 28th European Photovoltaic Solar Energy Conference* (2013) 1287.

[5] V. Jung and M. Köntges, Progress in Photovoltaics (2012) 876.

[6] V. Jung, F. Heinemeyer, M. Köntges and R. Brendel, Energy Procedia (2013) 362.

[7] W. P. Mulligan, M. J. Cudzinovic, T. Pass, D. Smith, and R. Swanson, US patent 7,388,147 B2.

[8] M. Kamp, J. Bartsch, G. Cimiotti, R. Keding, A. Zogaj, C. Reichel, A. Kalio, M. Glatthaar and S. Glunz, Solar Energy Materials & Solar Cells 120 (2014) 332.

[9] H. v. Campe, S. Huber, S. Meyer, S. Reiff and J. Vietor, *Proceedings of the 27th European Photovoltaic Solar Energy Conference* (2012) 1150.

[10] P. Schmitt, D. Eberlein, C. Ebert, M. Tranitz, U. Eitner and H. Wirth, Energy Procedia (2013) 380.

[11] www.schmid-group.com

[12] H. Schulte-Huxel, S. Blankemeyer, A. Merkle, V. Steckenreiter, S. Kajari-Schröder and R. Brendel, Progress in Photovoltaics 23 (2015) 1057.